*Power Electronics and Applications (EPE'19 ECCE-Europe), 2019 21th European Conference on*

# Flexible Medium Voltage DC Source Utilizing Series Connected Modular Multilevel Converters

M. Utvic, S. Milovanovic, and D. Dujic



POWER ELECTRONICS LABORATORY
ÉCOLE POLYTECHNIQUE FÉDÉRALE DE LAUSANNE

# Flexible Medium Voltage DC Source Utilizing Series Connected Modular Multilevel Converters

Milan Utvić, Stefan Milovanović, Dražen Dujić
Power Electronics Laboratory
École Polytechnique Fédérale de Lausanne
EPFL STI IEL PEL, Station 11
Lausanne, Switzerland
Phone: +41 21 693-4789
Email: milan.utvic@epfl.ch, stefan.milovanovic@epfl.ch, drazen.dujic@epfl.ch
URL: http://pel.epfl.ch

## Acknowledgments

This research project is part of the Swiss Competence Center for Energy Research SCCER FURIES of the Swiss Innovation Agency Innosuisse.

## Keywords

≪Multilevel Converter≫, ≪Voltage Source Converter≫, ≪DC Power Supply≫

## Abstract

This paper presents the converter configuration acting as a medium voltage DC source. In order to obtain desired voltage across the DC terminals, two series connected modular multilevel converters are used. The use of modular multilevel converters results in high degrees of modularity, flexibility, reliability, current limiting capability during DC faults, as well as the outstanding operational performances. Each modular multilevel converter is connected to the 3.3 kV AC supply, while ensuring arbitrary voltage in the range of $\pm$ 5 kV across its DC terminals. Consequently, series connection of two power units allows for $\pm$10 kV to be synthesized across the converter's DC terminals. Moreover, there is a freedom of choice with regards to the way that two modular multilevel converters share the output DC voltage reference. Therefore, studies focusing on converter dynamics and efficiency for various voltage sharing profiles are conducted. As a result, the most optimal voltage sharing profile is generated, covering the whole operating range of the converter.

## Introduction

High Voltage DC (HVDC) systems are nowadays considered mature and widely accepted technology for power transmission over the long distances or as means of connecting off-shore wind power plants with existing on-shore power grids. The driving force for its acceptance is higher efficiency compared to its AC counterparts, as well as the reduced system costs once the transmission distance exceeds the so-called break-even distance [1]. The same trend is expected in case of Medium Voltage (MV) and Low Voltage (LV) distribution grids due to a number of reasons [2]. Owing to the fact that urban areas are becoming more populated and congested, most of the distribution grids are nowadays realized using AC underground cables. It is identified that MV underground AC distribution cable link, normally ranging from 5-20 km in length and being responsible for bulk power delivery to the inner urban city substation, can benefit the most in terms of both capacity and efficiency enhancement, if the existing infrastructure is reused and operated under DC voltage [3].

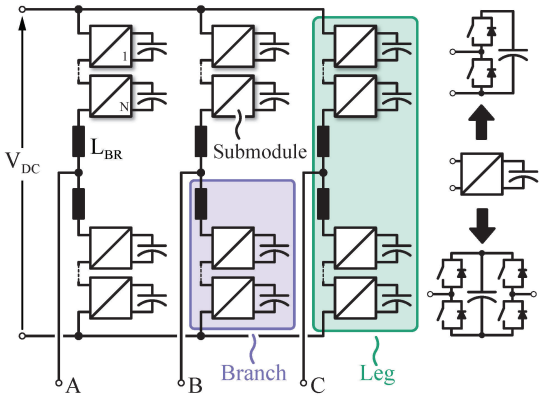


Fig. 1: Modular Multilevel Converter

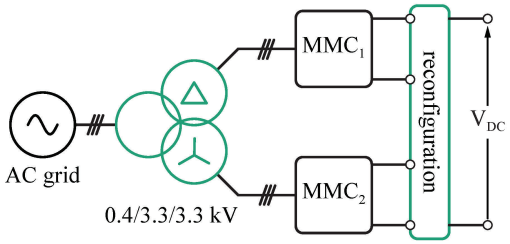


Fig. 2: Analyzed topology - Flexible and reconfigurable DC source

Potential of the MVDC distribution grids has been recognized in the marine applications as well. Namely, rectification of the ships generators' voltages removes the need for synchronous operation of the generators. However, the challenge of handling the DC faults has to be carefully addressed depending on the way the distribution is ensured [4].

Due to increasing interest in Medium Voltage DC (MVDC) technology, a need for MVDC source, able to emulate various conditions in MVDC grids also arises. Although still considered irreplaceable in the ultra High Voltage (HV) domain, conventional rectifiers utilizing diodes or thyristors suffer from several drawbacks. In the case of Diode Rectifier (DR), the output DC voltage is exclusively positive and uncontrollable, whereas in case of Thyristor Rectifier (TR), output DC voltage is controllable and can take both positive and negative values. However TR dynamics is limited by the line voltages zero crossings. Furthermore, both DR and TR normally require DC voltage filtering, as well as additional AC side chokes. One way of improving the DC voltage and AC current quality related to the aforementioned rectifiers is by using the Three-Phase (3PH) multiple secondaries transformer, with phase shifted secondary windings' voltages, therefore creating the multi-pulse rectifier. Nevertheless, the slow dynamics problem remains unresolved. An alternative to DR and TR in the MV domain can be found in the Active Front End (AFE) rectifiers, based on either two-level or multilevel topologies. Consequently, high operational dynamics is ensured, however with the limitation of providing exclusively positive DC voltage, with the minimum DC voltage being dependent on the grid voltage.

Modular Multilevel Converter (MMC) [5] utilizing Full-Bridge (FB) submodules (SMs) allows for voltage of both polarities to be generated across its DC terminals, with fast operational dynamics seen from both DC and AC terminals. During the last decade it has gained popularity in the field of HVDC [6], railway interties [7], [8], MV drives [9] and STATCOM applications [10]. More recent research activities regarding the MMC converter focus on its employment within the MVDC shipboard systems. The key driving factors are its increased reliability, as well as fault handling capability [11]. Namely, due to the fact that the MMC utilizing FB SMs is able to produce an arbitrary voltage of both polarities across its DC terminals with fast dynamics, it can counteract the DC short-circuit current.

Due to the number of drawbacks of DR and TR on one hand, various advantages of the MMC technology on the other, and due to the increased interest in application of the MMC in MVDC, this paper provides analysis of a twelve pulse transformer combined with two MMCs, as suggested in Fig. 2, with the aim of obtaining a highly flexible DC voltage source, operating with very fast dynamics. Specifically, series connection of the two MMCs, operated in the Voltage Source Mode (VSM) is subject of this paper analysis. Although not being essential in this type of converter, twelve pulse transformer with star-delta secondary windings is used due to its availability inside the laboratory. Such converter aims to serve as a testbed for various laboratory activities in the MVDC domain.

## Topology operating principles and control

MMC has been subject to various research topics, hence its dynamics and sizing have been well studied in the literature [12], [13]. Given that an MMC leg consists of two branches, with clusters of SMs being perceived as controllable voltage sources, a phase leg analysis can be performed through its decoupled AC and DC equivalent circuits. For the purpose of such analysis, two voltage components are generally introduced ((1)-(2)).

$$v_c = v_n + v_p \quad (1) \qquad v_s = \frac{v_n - v_p}{2} \quad (2)$$

The variable $v_c$ is also being referred as a leg common voltage, and is coupled with the MMC equivalent DC circuit. The other voltage component $v_s$, also referred to as differential voltage, is being accounted for the converter AC analysis. As a consequence of two decoupled voltage components, two current components are present as well, with their relation to branch currents being presented in (3)-(4). Current component $i_C$ denotes the so-called circulating current, whereas $i_{AC}$ denotes the grid current [12]. Owing to the decoupled nature of the two systems, which can be noticed from Fig. 3, two current components can be controlled independently from each other.

$$i_p = i_C + \frac{i_{AC}}{2} \quad (3) \qquad i_n = i_C - \frac{i_{AC}}{2} \quad (4)$$

Since all the legs of a 3PH MMC share the same DC link, by observing Fig. 3, it is easy to derive the circuit depicted in Fig. 4, that represents the MMC seen from its DC terminals. This circuit indicates that mean value of the voltage across MMC DC terminals matches the $v_c^{(i)}$ average (zero) component, further denoted as $v_{c,0}$. The inductive voltage drop does not exist in the steady state, due to the nature of the output current, whereas the branch resistance can be neglected, and consequently its corresponding voltage drop. Therefore, by controlling the voltage $v_{c,0}$, steady state value of the DC link voltage $V_{DC}$ is being adjusted as well.

In the configuration being analyzed, DC links of the two MMCs are connected in series, with the purpose of realizing Flexible DC Source (FlexDCS). Both converters can be operated either in the VSM or in the Current Source Mode (CSM) [14], yet the paper is focused exclusively on the VSM. Due to the fact that FB SMs are used within both MMCs, DC voltage of both polarities can be generated across converter's DC terminals, according to (1)-(2). Moreover, voltage components $v_{c,0}$ of the two MMCs can be freely

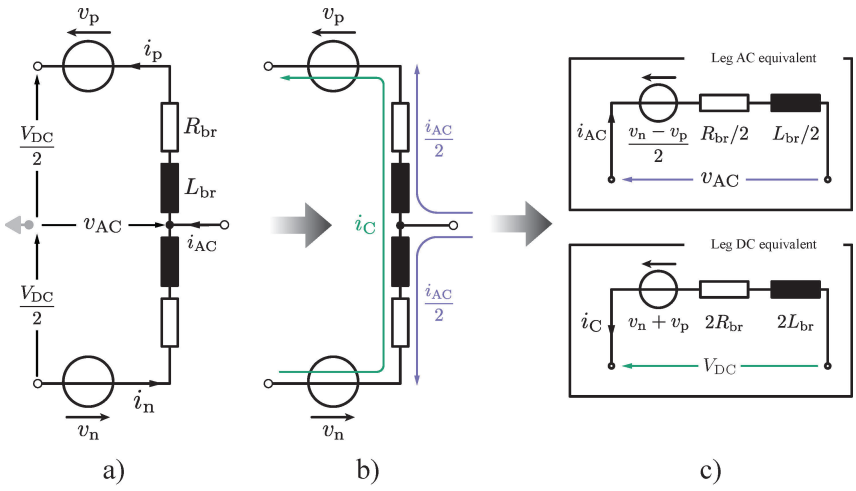


Fig. 3: Derivation of a leg equivalent circuit; a) MMC leg with the clusters of SMs being presented in the form of ideal voltage sources. Upper and lower branch voltages and currents are denoted with subscripts "p" and "n", respectively; b) Leg current components: circulating current ($i_C$), and AC grid current ($i_{AC}$); c) AC and DC equivalent circuits.

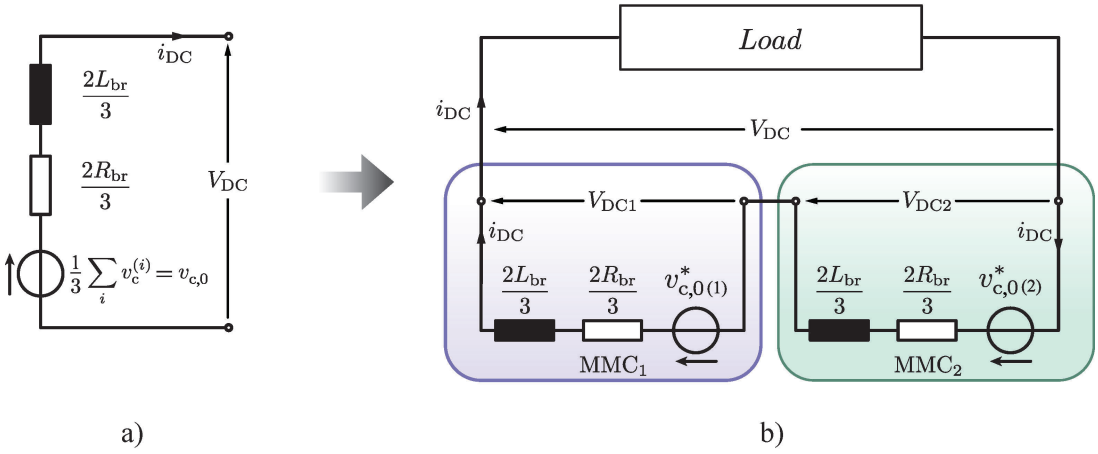


Fig. 4: Equivalent DC representation of a) Single MMC b) FlexDCS

adjusted so as to sum up to the desired output DC voltage, with insignificant delay depending on the system sampling frequencies, thus providing the basis for excellent dynamic performance.

Control of the output DC voltage can be organized in the closed-loop manner, as suggested in [15], where two control loops are introduced. The inner control loop takes care of the DC current control, whereas the outer control loop is added so as to compensate for the inner voltage drop. Nevertheless, this paper considers the output DC voltage control organized in an open-loop manner, as presented in Fig. 5. Each MMC is being separately fed with its DC voltage reference $V^*_{DC(x)}$, whereas the inner voltage drop is being compensated by the feedforward action. The main reason for this kind of approach lies within the fact that the expected inner voltage drop is predictable and accounts for less than 1 % of the nominal output DC voltage. Constants $k_1$ and $k_2$ are determined according to (5)-(6), where variables $\overline{V_F}$ and $\overline{R_{on}}$ refer to the mean values of the IGBT's and reverse diode's forward voltage drop and on-state resistance, respectively. Therefore, the open-loop voltage control, together with feedforward inner voltage drop compensation is the way to avoid having two control loops, and consequently ensure fast dynamics.

$$k_1 = 4N\overline{V_F} \qquad (5) \qquad k_2 = \frac{2}{3}(2N\overline{R_{on}} + R_{br}) \qquad (6)$$

Control concept introduced in this paper also features short-circuit protection, implemented in a way presented in Fig. 5. Namely, once the measured current exceeds the threshold value, CSM is activated,

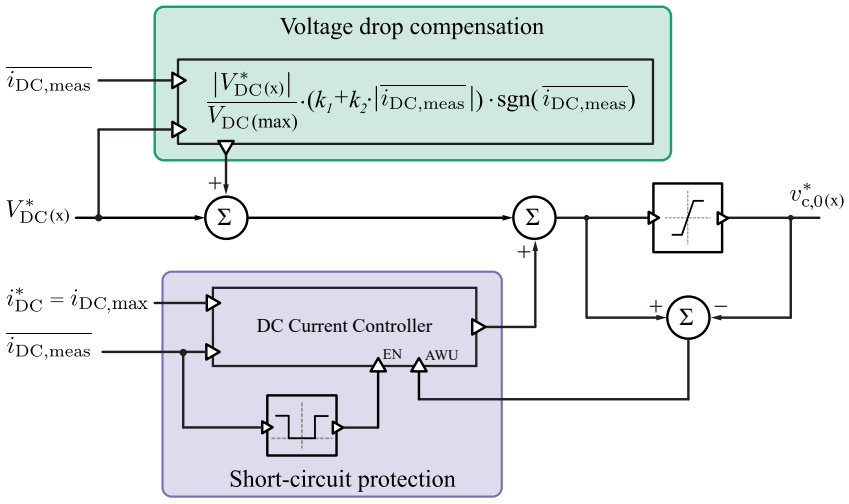


Fig. 5: Output DC voltage control block diagram of a single MMC. Both MMCs are controlled independently.

Table I: Simulated FlexDCS parameters

| Number of SMs/branch | SM switching frequency [Hz] | Rated power [kW] | Max. DC voltage [kV] |
|---|---|---|---|
| 8 | 1000 | 500 | $\pm$ 10 |

with the objective of limiting the output DC current to the maximum permissible value. Only when the output current drops below the maximum value, does the converter resume into the VSM operation. Both converters perform their internal control independently from each other, whereas the output DC voltage reference is supplied from the upper level control to each one of them. In that sense, there is a freedom of choice with regards to the way that two MMCs share the output DC voltage, which is the subject of this paper.

It is clear that SMs voltage mean value needs to be maintained at a desired reference, such that AC side currents can be controlled irrespectively of the DC voltage reference. Although not presented in the paper, horizontal and vertical balancing of both MMCs are implemented in the $\alpha\beta$ domain, according to [16], whereas the total energy balancing is obtained through AC currents control, implemented in the $dq$ domain. With the aim of generating voltages whose average over a chosen period corresponds to the desired references, Phase-Shifted Carriers (PSC) modulation [17] is selected for the implementation.

## Output DC Voltage Sharing Impact on Converter Output Dynamics

FlexDCS configuration was simulated in PLECS with the aim of validating employed control principles. Simulation parameters can be found in Table I. Converter was loaded with the resistive load, whose power consumption at maximum attainable DC voltage corresponds to the converter rated power, according to Table I. To test the converter operation, different output DC voltage references were set in different time instants, while the voltage reference was equally shared among the two MMCs. Fig. 6 presents $\text{MMC}_1$ relevant current and voltage waveforms. Due to the waveforms similarities, $\text{MMC}_2$ waveforms were not presented. Please notice that, despite abrupt reference and load power changes, the

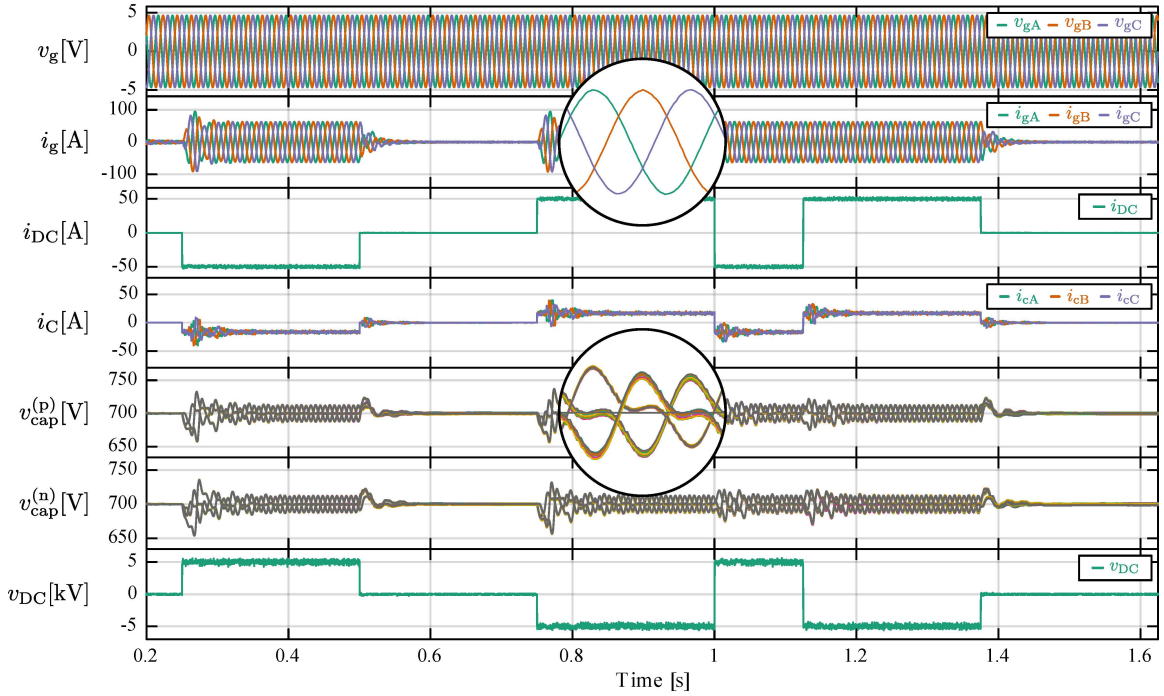


Fig. 6: $\text{MMC}_1$ relevant waveforms. From top to bottom: $v_g$ - AC grid voltages; $i_g$ - AC grid currents; $i_{DC}$ - output DC current; $i_C$ - circulating currents; $v_{cap}^{(p)}$ - upper branch SMs' voltages; $v_{cap}^{(n)}$ - lower branch SMs' voltages; $v_{DC}$ - output DC voltage.

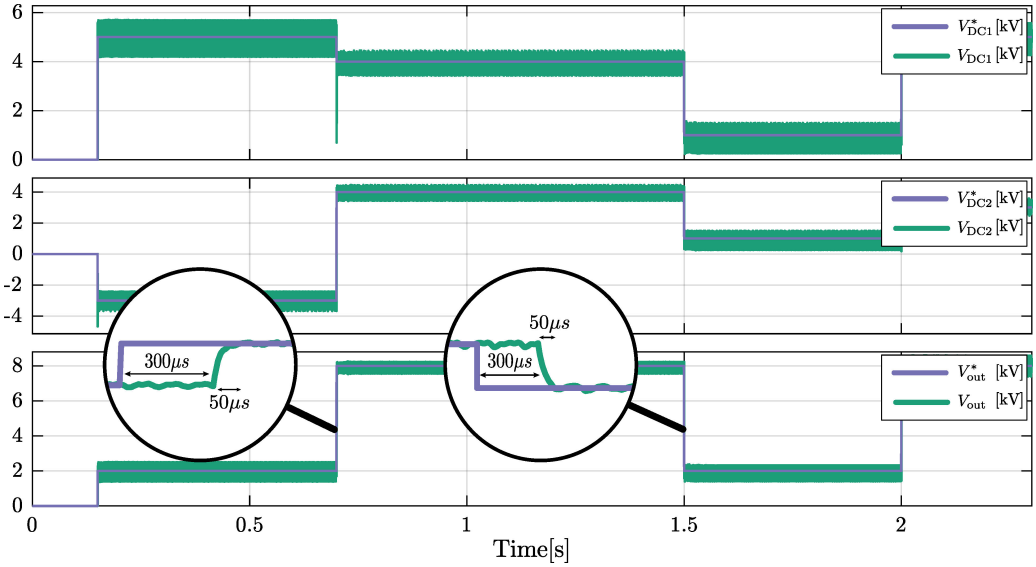


Fig. 7: Dynamic response of the converter for various voltage sharing profiles

observed MMC stays balanced at all times.

However, owing to the fact that each MMC is able to provide an arbitrary DC voltage in the range of $\pm 5\,\mathrm{kV}$, there is a degree of freedom with regards to the way that the two converters share the output DC voltage reference. At first, the simulation aimed at inspecting the dynamics of the FlexDCS voltage generation for various voltage sharing profiles was performed (c.f. Fig. 7). The output DC voltage reference was changed from 2 kV to 8 kV and vice versa, with the references being unequally distributed between the two MMCs. The load considered during this simulation was resistive load, as in the previous simulation. Simulation results show that in terms of the output DC voltage dynamics, observed through the output DC voltage rise time, there exists no difference between different reference distributions among the MMCs. Output DC voltage dynamics is solely determined by the delays, attributed to computational and sampling delays, as well as the time constant of the equivalent circuit presented in Fig. 4. Nevertheless, converter efficiency might vary with different voltage references being shared between the two MMCs, owing to the fact that single MMC converter might experience different power losses for different output DC voltages. Therefore, it is beneficial to perform an analysis that focuses on determining the voltage sharing profile between the two MMCs, with the aim of minimizing converter power losses.

## Output DC Voltage Sharing Impact on Converter Power Losses

In order to map the power losses of a single MMC throughout its complete operating range, its Safe Operating Area (SOA) needs to be determined. It has already been stated that the output DC voltage of a single MMC ranges from $-5\,\mathrm{kV}$ to $5\,\mathrm{kV}$. Regarding the power ratings, single MMC is sized for the rated power of 250 kW. Converter currently being developed employs IGBTs rated for the maximum continuous current of 50 A, which is further on being labeled as $I^{\max}_{\mathrm{IGBT}}$. Current through a single IGBT is defined with (7), where $I_{\mathrm{AC}}$, $I_{\mathrm{DC}}$, $\Delta I_{\mathrm{bal}}$ refer to the grid rms current, DC output current and balancing current components, respectively. Considering balancing components to be lower than 20 % of the maximum IGBT current, equalizing equations (8) and (9) yields the maximum permissible output DC current ($I^{\max}_{\mathrm{DC}}$) as a function of the output DC voltage ($V_{\mathrm{DC}}$) and rated IGBT current ($I^{\max}_{\mathrm{IGBT}}$), given in (10).

$$I_{\mathrm{IGBT}} = \frac{I_{\mathrm{AC}}}{2} + \frac{I_{\mathrm{DC}}}{3} + \Delta I_{\mathrm{bal}} \qquad (7) \qquad P_{\mathrm{DC}} = V_{\mathrm{DC}} I_{\mathrm{DC}} \qquad (8) \qquad P_{\mathrm{AC}} = \sqrt{3} V_{\mathrm{AC}} I_{\mathrm{AC}} \qquad (9)$$

$$I^{max}_{\mathrm{DC}} = \left(0.8 I^{\max}_{\mathrm{IGBT}}\right)\left(\frac{1}{3} + \frac{V_{\mathrm{DC}}}{2\sqrt{3} V_{\mathrm{AC}}}\right)^{-1} \qquad (10)$$

Simulations aiming to map the power losses of a single MMC throughout the whole SOA are performed in PLECS. SOA is divided into the mesh covering 21 different output DC voltages and 21 different output DC currents, and each of these operating points was simulated. Each MMC SM [18] consists of a single H-bridge IGBT module [19], as well as the bank of electrolytic capacitors [20]. Converter power losses of interest are the switching, conduction and reverse recovery losses within the H-bridge IGBT modules, as well as the power losses within electrolytic capacitors. Other types of losses, such as the conduction losses within the branch air-core inductances are neglected in this analysis.

Simulation results are collected, processed and the power losses of a single MMC, as a function of the output DC voltage and the output DC current, are presented in Fig. 8. Each of the intersections represents the power losses in a given operating point, and such 3-D matrix can be used as an input to the algorithm that determines the most efficient voltage sharing profile. Algorithms of this kind can be implemented as part of the converter control software, with real time execution, or offline, with the result being generated in a form of a look-up table.

Offline algorithm for calculation of the most efficient voltage reference distribution among the MMCs is implemented in MATLAB, and the results are presented in Fig. 9. The final result of the algorithm is the look-up table, with input variables being the converter output DC voltage and output DC current. Output value of the look-up table is the optimal voltage reference for a single MMC converter, whereas the voltage reference of another MMC complements to the total output DC voltage reference. Fig. 9 is the graphical representation of the generated look-up table. Generated look-up table contains only positive values of the output DC voltage reference, but it can be applied for the negative references as well, due to the symmetry. In addition, SOA of the FlexDCS is restricted to 50 A, due to the fact that the maximum permissible output DC current of a single MMC differs throughout the voltage range (c.f. Fig. 8). Therefore, choice of the 50 A represents the maximum common value of the DC current for two MMCs, throughout the whole output DC voltage range.

Inspection of the look-up table shows that the voltage reference of a single MMC that ensures minimum power losses, closely corresponds to the case when the reference is shared equally among the two MMCs. Therefore, it is beneficial to determine to what extent do the power losses of the FlexDCS with the optimal DC voltage reference distribution, differ from the power losses in case when the MMCs are equally loaded. Fig. 10 shows the difference between the power losses in case of optimal and equal DC voltage reference distribution. It can be observed that the difference in terms of power losses exists, however it is not significant. This leads to the conclusion that the FlexDCS can operate with equal voltage reference sharing, without significantly compromising efficiency. Given that both MMCs operate with equal voltage reference sharing, both MMCs can handle the same current at a given DC voltage, therefore the SOA of the FlexDCS can be extended as presented in Fig. 11.

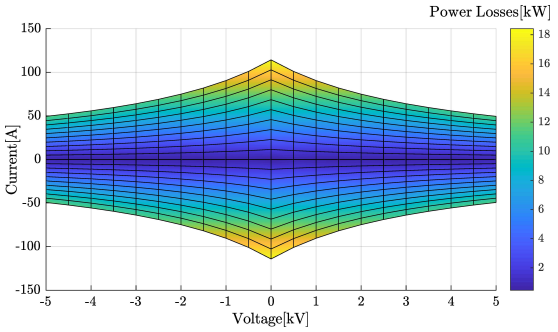


Fig. 8: Power losses distribution throughout the whole SOA of a single MMC

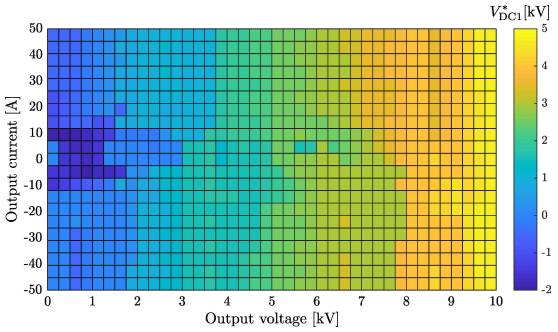


Fig. 9: Graphical representation of the generated look-up table

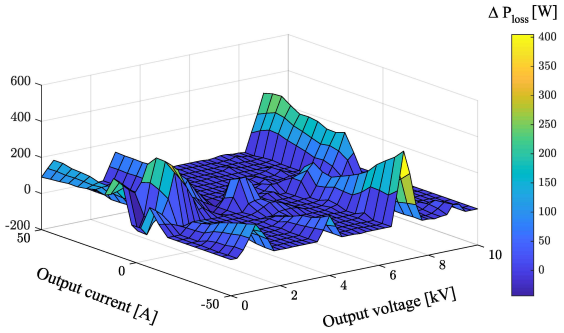


Fig. 10: Power losses reduction with the optimal voltage reference sharing compared to the equally loaded MMCs

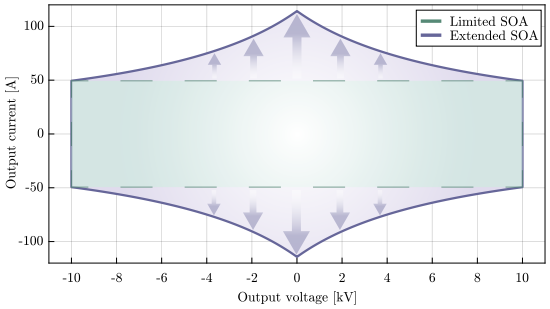


Fig. 11: SOA extension of the FlexDCS in case of equal voltage reference distribution

## Conclusion

This paper presents MMC-based topology intended to operate as a flexible MVDC source. The use of the MMC employing FB SMs enables realization of both positive and negative voltage across the converter's DC terminals, which is a useful property in handling DC short circuit currents. Control of such converter is presented, together with application dedicated open-loop output DC voltage control. Converter is simulated for various output DC voltage reference profiles, and shows excellent operating dynamics, while keeping all the energy states within the MMCs around their references.
Due to the freedom of choice of the output DC voltage reference distribution, studies aimed at inspecting the converter dynamics for different output DC voltage sharing profiles were conducted, showing that the output DC voltage dynamics is not affected by an arbitrary voltage sharing. Safe operating area of a single MMC is defined, and power losses are assessed by means of PLECS simulations and proper tools developed in MATLAB. The results are further used to determine the most efficient voltage sharing profile between the converters. As a result, a look-up table with the optimal voltage reference distribution is generated and presented. Results demonstrate that the optimal voltage distribution is to great extent close to the case when the references are shared equally. In addition, power losses in case of the optimal and equal voltage reference distribution are compared and presented, showing that the difference is not significant, and thus FlexDCS can operate equally sharing the output voltage references between the two MMCs without compromising efficiency.

## References

[1] S. Lundberg, *Wind farm configuration and energy efficiency studies-series DC versus AC layouts*. Chalmers University of Technology, 2006.

[2] D. Boroyevich, I. Cvetkovic, R. Burgos, and D. Dong, "Intergrid: A future electronic energy network?", *IEEE Journal of Emerging and Selected Topics in Power Electronics*, vol. 1, no. 3, pp. 127–138, Sep. 2013.

[3] A. Shekhar, E. Kontos, A. R. Mor, L. Ramírez-Elizondo, and P. Bauer, "Refurbishing existing mvac distribution cables to operate under dc conditions", in *2016 IEEE International Power Electronics and Motion Control Conference (PEMC)*, Sep. 2016, pp. 450–455.

[4] U. Javaid, F. D. Freijedo, D. Dujic, and W. van der Merwe, "Dynamic assessment of source–load interactions in marine mvdc distribution", *IEEE Transactions on Industrial Electronics*, vol. 64, no. 6, pp. 4372–4381, Jun. 2017.

[5] A. Lesnicar and R. Marquardt, "An innovative modular multilevel converter topology suitable for a wide power range", in *2003 IEEE Bologna Power Tech Conference Proceedings,*, vol. 3, Jun. 2003, 6 pp. Vol.3-.

[6] S. P. Teeuwsen, "Modeling the trans bay cable project as voltage-sourced converter with modular multilevel converter design", in *2011 IEEE Power and Energy Society General Meeting*, Jul. 2011, pp. 1–8.

[7] M. Winkelnkemper, A. Korn, and P. Steimer, "A modular direct converter for transformerless rail interties", in *2010 IEEE International Symposium on Industrial Electronics*, Jul. 2010, pp. 562–567.

[8] D. Weiss, M. Vasiladiotis, C. Banceanu, N. Drack, B. Odegard, and A. Grondona, "Igct based modular multilevel converter for an ac-ac rail power supply", in *PCIM Europe 2017; International Exhibition and Conference for Power Electronics, Intelligent Motion, Renewable Energy and Energy Management*, May 2017, pp. 1–8.

[9] D. Krug, S. Busse, and M. Beuermann, "Complete performance test of mv drive with modular multilevel topology for high power oil amp; gas applications", in *2016 Petroleum and Chemical Industry Technical Conference (PCIC)*, Sep. 2016, pp. 1–6.

[10] J. Park, S. Yeo, and J. Choi, "Development of ±400mvar world largest mmc statcom", in *2018 21st International Conference on Electrical Machines and Systems (ICEMS)*, Oct. 2018, pp. 2060–2063.

[11] T. A. Toshon, A. Newaz, and M. O Faruque, "Fault current limiting capabilities of tcr and mmc for mvdc based shipboard power systems", Apr. 2018.

[12] L. Harnefors, S. Norrga, A. Antonopoulos, and H.-P. Nee, "Dynamic modeling of modular multilevel converters", in *Power Electronics and Applications (EPE 2011), Proceedings of the 2011-14th European Conference on*, IEEE, 2011, pp. 1–10.

[13] K. Ilves, S. Norrga, L. Harnefors, and H.-P. Nee, "On energy storage requirements in modular multilevel converters", *IEEE Transactions on Power Electronics*, vol. 29, no. 1, pp. 77–88, 2014.

[14] M. M. Steurer, K. Schoder, O. Faruque, D. Soto, M. Bosworth, M. Sloderbeck, F. Bogdan, J. Hauer, M. Winkelnkemper, L. Schwager, and P. Blaszczyk, "Multifunctional megawatt-scale medium voltage dc test bed based on modular multilevel converter technology", *IEEE Transactions on Transportation Electrification*, vol. 2, no. 4, pp. 597–606, Dec. 2016.

[15] P. Blaszczyk, M. Steurer, D. Soto, M. Bosworth, and M. Winkelnkemper, "Power balancing in multi-converter systems composed of modular multilevel converters (mmcs)", in *2016 18th European Conference on Power Electronics and Applications (EPE'16 ECCE Europe)*, Sep. 2016, pp. 1–10.

[16] F. Kammerer, J. Kolb, and M. Braun, "Fully decoupled current control and energy balancing of the modular multilevel matrix converter", in *Power Electronics and Motion Control Conference (EPE/PEMC), 2012 15th International*, IEEE, 2012, LS2a–3.

[17] K. Ilves, L. Harnefors, S. Norrga, and H.-P. Nee, "Analysis and operation of modular multilevel converters with phase-shifted carrier PWM", *IEEE Transactions on Power Electronics*, vol. 30, no. 1, pp. 268–283, 2015.

[18] M. Utvic, I. Polanco, and D. Dujic, "Low voltage modular multilevel converter submodule for medium voltage applications", in *PCIM Europe 2019; International Exhibition and Conference for Power Electronics, Intelligent Motion, Renewable Energy and Energy Management*, May 2019, pp. 1–8.

[19] Semikron. (23-03-2016). SK50GH12T4T datasheet, [Online]. Available: `https://www.semikron.com/dl/service-support/downloads/download/semikron-datasheet-sk-50-gh-12t4-t-24915220.pdf`.

[20] Exxelia. (9/2017). Exxelia Sic Safco. SNAPSIC 4P datasheet, [Online]. Available: `http://www.exxelia.com/uploads/PDF/snapsic-4p-v1.pdf`.